Comparison of Side-On and End-On Coordination of E_2 Ligands in Complexes $[W(CO)_5E_2]$ (E = N, P, As, Sb, Bi, Si^-, Ge^-, Sn^-, Pb^-)**

Catharine Esterhuysen*[a, b] and Gernot Frenking*[a]

Dedicated to Professor Helmut Schwarz on the occasion of his 60th birthday

Abstract: Complexes of $W(CO)_5$ with neutral diatomic pnictogen ligands N_2, P_2, As_2, Sb_2, and Bi_2 and anionic Group 14 ligands Si_2^{2-}, Ge_2^{2-}, Sn_2^{2-}, and Pb_2^{2-} coordinated in both side-on and end-on fashion have been optimized by using density functional theory at the BP86 level with valence sets of TZP quality. The calculated bond energies have been used to compare the preferential binding modes of each respective ligand. The results were interpreted by analyzing the nature of the interaction between the ligands and the metal fragment using an energy partitioning method. This yields quantitative information regarding the strength of covalent and electrostatic interactions between the metal and ligand, as well as the contributions by orbitals of different symmetry to the covalent bonding. Results show that all the ligands studied bind preferentially in a side-on coordination mode, with the exception of N_2, which prefers to coordinate in an end-on mode. The preference of the heavier homologues P_2–Bi_2 for binding in a side-on mode over the end-on mode in the neutral complexes $[(CO)_5WE_2]$ comes mainly from the much stronger electrostatic attraction in the former species. The energy difference between the side-on and end-on isomers of the negatively charged complexes with the ligands Si_2^{2-}, Ge_2^{2-}, Sn_2^{2-}, and Pb_2^{2-} is much less and it cannot be ascribed to a particular bonding component.

Keywords: bonding analysis · coordination modes · density functional calculations · Group 14 elements · pnicogens

Introduction

Heavier element homologues of dinitrogen, that is P_2, As_2, Sb_2, and Bi_2 are only found as free molecules at high temperatures in the gas phase.[1] These molecules can, however, be stabilized by coordination to two or more organometallic species, typically metal carbonyl compounds, in a variety of different ways.[2] The diatomic ligands, in particular As_2, are able to act formally as four-, six-, or even eight-electron donor species,[2d] primarily by side-on coordination to metal species. The bonding behavior of the heavier homologues is substantially different to that of N_2 which preferentially binds in an end-on manner to a single metal center,[3] although a number of examples of two metal fragments both coordinating end-on have been reported.[4] Side-on coordination of N_2 to a single organometallic fragment has been postulated for transition states in intramolecular N exchanges,[5] however only one example of a photo-induced metastable complex with N_2 coordinated in a side-on manner has been structurally characterized.[6] A few complexes containing N_2 coordinated side-on to two organometallic fragments have also been characterized by X-ray crystallography.[4c, 7]

Despite the fact that the ligands P_2–Bi_2 serve many-electron donors in numerous complexes, the P–P, As–As, Sb–Sb, and Bi–Bi separations are still considerably shorter than in the respective single bonds. In the case of As_2 this short bond length has been attributed to a high degree of multiple-bond character,[8] where it is assumed that the electron donation and back-bonding interactions result in a decrease in bond order from 3 (in the free state) to 2 in the complex. This was proposed to result from a decrease in the π-bonding order from 2 to 1, by (a) electron donation from filled π orbitals on As_2 to metal orbitals and (b) back-donation of electron density from the metal center to empty π^* orbitals on As_2. It was thus concluded that both processes occur synergistically, yielding no net charge-transfer. It has also been suggested[2a] that in the complex $[Co_2(CO)_6As_2]$ the $Co(CO)_3$ groups can be regarded as "electron sinks", removing electron density from the diarsenic fragment. The result-

[a] Dr. C. Esterhuysen, Prof. G. Frenking
Fachbereich Chemie, Philipps-Universität Marburg
Hans-Meerwein-Strasse, 35042 Marburg (Germany)
Fax: (+49)6421-2825566
E-mail: frenking@chemie.uni-marburg.de

[b] Dr. C. Esterhuysen
Department of Chemistry, Stellenbosch University,
Matieland, 7602, South Africa

[**] Theoretical Studies of Inorganic Compounds. Part 29. Part 28: M. Lein, A. Szabo, A. Kovács, V.M. Rayón, G. Frenking, *Disc. Faraday Soc.* in press.

DOI: 10.1002/chem.200304723

ing reduction in electron pair repulsions within the As_2 ligand then yield the significantly shorter As–As bonds observed.

Campana et al.[9] reached a similar conclusion when studying the isostructural and isoelectronic $[Co_2(CO)_5\{P(C_6H_5)_3\}P_2]$ complex. In this example, a bond length to valence bond order curve was available for P_2, which was employed to determine a bond order of 2 for the diphosphorus ligand in the complex. A reduction in π bond order was determined to be the reason for this. It has been proposed that in "star-type" complexes, in which three $W(CO)_5$ fragments coordinate to As_2, Sb_2, or Bi_2 (which thus act as six-electron donors), electron donation takes place not only from the π orbitals, but also from the σ orbitals.[2d] A theoretical calculation of the bond situation in $[W(CO)_5As_2]$ by using extended Hückel theory[2e] showed that the good π-acceptor ability of the As_2 molecule assists the complex formation, since the presence of a weak As–As π bond results in a low-energy π* orbital, which can easily overlap with the d orbitals on tungsten. The As–As σ bond was also found to be weak, with a correspondingly high energy level, thus allowing bonding to the metal fragment. The Dewar–Chatt–Duncanson model was therefore not utilized for describing the bonding in $[\{W(CO)_5\}_3As_2]$.

The behavior of the Group 15 diatomic molecules E_2 (E = P–Bi) as ligands in transition-metal complexes is also found for the isoelectronic Group 14 diatomic dianions E_2^{2-} (E = Si–Pb). For example, the recent synthesis of a complex which is analogous to $[\{W(CO)_5\}_3As_2]$ containing the valence isoelectronic Pb_2^{2-} fragment coordinated to four $W(CO)_5$ fragments (three side-on coordinated fragments in star-type coordination mode and one end-on coordinated fragment) leads to a structure whose Pb–Pb bond length is also very short, despite the Pb_2^{2-} ligand acting as an eight-electron donor.[10]

The experimental observations pose important questions about the bonding situation in complexes of diatomic ligands of Group 14 and Group 15 elements, which have not been answered with modern quantum-chemical methods. What is the reason that N_2 bonds preferentially in an end-on manner, while the heavier homologues P_2–Bi_2 prefer side-on coordination? What is the difference in the bonding situation between the Group 15 ligands and the isoelectronic Group 14 dianions in transition-metal complexes? What is the nature of the metal–E_2 interactions in terms of covalent and electrostatic bonding and which orbitals are involved? What is the theoretically predicted bond dissociation energy of the ligands? What is the strength of the metal ← E_2 donation and the metal → E_2 back-donation? An additional interesting point is that star-type complexes containing lighter homologues of As_2 and Pb_2^{2-} have not yet been observed experimentally.

To answer these questions, it was decided to first study how one $W(CO)_5$ fragment interacts with neutral dinitrogen (**1**), diphosphorus (**2**), diarsenic (**3**), diantimony (**4**), and dibismuth (**5**) ligands, in both the side-on (**1s**–**5s**) and end-on (**1e**–**5e**) coordinated modes. For comparison the uncoordinated E_2 molecules (**1**–**5**) were also calculated. Furthermore, calculations were also performed on complexes containing the isoelectronic homologues of **1**–**5**: dianionic carbon (**6**), disilicon (**7**), digermanium (**8**), ditin (**9**), and dilead (**10**). However, for the dicarbon homologue it proved impossible to obtain stable minima with the same side-on and end-on structures as the remainder of the complexes. The calculated structures of $[(CO)_5W(C_2)]^{2-}$ will be reported in a separate paper. A discussion of **6**, **6s**, and **6e** will thus not be included in this work. This work lays the foundation for an understanding of the metal–ligand bonding of the ligands E_2 (E = N–Bi) and E_2^{2-} (E = Si–Pb) in mononuclear complexes $[(CO)_5W(E_2)]$ and $[(CO)_5W(E_2)]^{2-}$. Our work is the first quantum-chemical investigation at the DFT or ab initio level of theory of the molecules, except for the dinitrogen species **1s** and **1e** which have been reported before.[11] In a future study we will report the oligonuclear complexes $[\{W(CO)_5\}_nE_2]$ and $[\{W(CO)_5\}_nE_2]^{2-}$ $(n = 2–5)$.

Computational Methods

The calculations were performed at the nonlocal DFT level of theory using the exchange functional of Becke[12] and the correlation functional of Perdew[13] (BP86). Calculations were performed with the programs Gaussian98[14] and/or ADF-2000.02.[15] The reason for choosing two programs is that Gaussian98 has analytical second derivatives that make the calculation of the vibrational frequencies much more efficient than with ADF which has only numerical second derivatives. On the other hand, the energy decomposition analysis can only be carried out with ADF.

In the Gaussian calculations the basis sets used for C and O were 6-31G(d) for neutral complexes, and 6-31 + G(d) for the anionic complexes. LANL2DZ[16] was used for W. Stuttgart basis sets[17] with effective core potentials and one polarization function (Huzinaga[18] where available;[19] for N ($\zeta = 0.853$), P ($\zeta = 0.380$), and Si ($\zeta = 0.276$) the exponents of the polarization functions were optimized by using numerical interpolation of the calculated atomic energies at CISD level, according to the method of Höllwarth et al.[20]) were used for N, P, As, Sb, Bi, Si, Ge, Sn, and Pb. One set of diffuse s and p functions were added to Si ($\zeta_s = 0.02899$; $\zeta_p = 0.02383$), Ge ($\zeta_s = 0.02134$; $\zeta_p = 0.0204$), Sn ($\zeta_s = 0.02484$; $\zeta_p = 0.01566$), and Pb ($\zeta_s = 0.0238$; $\zeta_p = 0.01635$); the exponents ($\zeta_{diffuse}$) were determined following the method suggested by Lee and Schaefer[21] [Eq. (1)], where L, $L-1$, and $L-2$ are the last, second last, and third last exponents of the primitive set respectively. This level of theory is denoted as BP86/LANL2DZ(+).

$$\zeta_{diffuse} = \tfrac{1}{2}\left(\frac{L}{L-1} + \frac{L-1}{L-2}\right)L \qquad (1)$$

In ADF triple-ζ basis sets augmented with one polarization function were used for all atoms. Relativistic effects were included by using the ZORA formalism.[22] One set of diffuse s and p functions were added for anionic complexes to C, O, Si, Ge, Sn, and Pb; diffuse coefficients for C and O were taken from Guan et al.,[23] diffuse coefficients for Si ($\zeta_s = 0.75$; $\zeta_p = 0.50$), Ge ($\zeta_s = 0.7875$; $\zeta_p = 0.4668$), Sn ($\zeta_s = 0.887$; $\zeta_p = 0.527$), and Pb ($\zeta_s = 1.033$; $\zeta_p = 0.572$) were added to the existing basis set in an even-tempered way, similar to that described above. This level of theory is denoted as BP86/TZP. The values in the paper refer to calculations at BP86/TZP unless otherwise specified.

Geometry optimizations were performed with both Gaussian 98[14] and ADF-2000.02.[15] Vibrational frequency calculations at BP86/LANL2DZ(+) were used to confirm that minimum energy conformations had been achieved, natural bond orbital (NBO) analysis (as implemented in Gaussian98)[24] yielded atomic charges and bond orders. The bonding interactions between the E–E molecules and the $W(CO)_5$ fragment were determined using the energy decomposition method in ADF.[20a] In this method the instantaneous interaction energy (ΔE_{int}) between the two fragments can be divided into three components [Eq (2)], where ΔE_{elstat}

$$\Delta E = \Delta E_{elstat} + \Delta E_{Pauli} + \Delta E_{orb} \qquad (2)$$

gives the electrostatic interaction energy between the fragments, calculated with a frozen electron density distribution in the geometry of the complex.

ΔE_{Pauli} gives the repulsive four-electron interactions between occupied orbitals and ΔE_{orb} gives the stabilizing orbital interactions. Since ΔE_{orb} can be considered as an estimate of the covalent contributions to the bonding the ratio of $\Delta E_{elstat}/\Delta E_{orb}$ indicates the electrostatic or covalent nature of the bond. Furthermore, the contributions of σ and π bonding to a covalent multiple bond can be determined by partitioning the ΔE_{orb} term into the contributions by orbitals that belong to different irreducible representations of the interacting system.

The bond dissociation energy ΔE_e can be determined from ΔE_{int} and the fragment preparation energy ΔE_{prep}, which is the energy necessary to promote fragments from their equilibrium geometry and electronic ground state to the geometry and electronic state of the optimized structure [Eq. (3)].

$$\Delta E_e = \Delta E_{prep} + \Delta E_{int} \quad (3)$$

Results and Discussion

Neutral molecules (1s–5s, 1e–5e, 1u–5u): Geometry optimization of the $W(CO)_5$ complexes with neutral E_2 ligands revealed that the minimum energy conformation for side-on coordination has an eclipsed C_{2v} symmetry, whereas complexes containing E_2 fragments in the end-on coordination mode have C_{4v} symmetry minimum energy conformations (Figure 1). Selected geometrical parameters from the optimization of the side-on (**1s–5s**) and end-on (**1e–5e**) coordination modes, as well as for the uncoordinated molecules (**1–5**), are listed in Table 1.

The E–E bond lengths in the neutral free molecules compare quite well with available experimental values

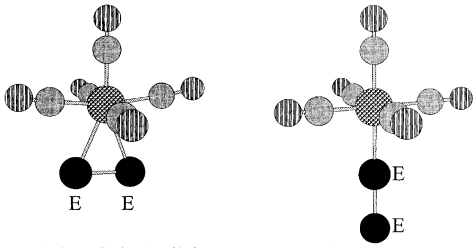

E = N (**1s**), P (**2s**), As (**3s**), Sb (**4s**), Bi (**5s**), Si^- (**7s**), Ge^- (**8s**), Sn^- (**9s**), Pb^- (**10s**)

E = N (**1e**), P (**2e**), As(**3e**), Sb (**4e**), Bi (**5e**), Si^- (**7e**), Ge^- (**8e**), Sn^- (**9e**), Pb^- (**10e**)

Figure 1. Schematic representation of the $W(CO)_5$ complexes with neutral and anionic ligands showing the C_{2v} symmetry of the side-on coordination mode and the C_{4v} symmetry of the end-on coordination mode.

(N–N: 1.098 Å;[25] P–P: 1.893 Å;[25] As–As: 2.103 Å;[25] Sb–Sb: 2.48 Å;[26] Bi–Bi: 2.660 Å[25]), and previously calculated theoretical results (N–N: 1.106 Å;[27] P–P: 1.894 Å;[28] As–As: 2.164 Å;[29] Sb–Sb: 2.58 Å;[29] Bi–Bi: 2.79 Å[29]). The calculated values of the heavier species As_2, Sb_2, and Bi_2 at BP86/LANL2DZ(+) agree better with the experimental data than BP86/TZP but both methods predict very similar changes of the interatomic distances E–E in the complexes The only calculated E–E bond lengths in complexes that can be compared to experimental results are the N–N distances in **1s** and **1e**. In **1s** this distance is calculated with both methods as 1.129 Å, which is longer than the only experimentally determined side-on coordinated N–N bond length of 1.058(30) Å in the complex $Os(NH_3)_5(\eta^2\text{-}N_2)$.[6] However, the authors of this paper point out that the observed shortening is not significant, considering the large estimated standard deviation of the bond length, and the fact that the bond is between two light atoms in the close proximity of the heavy Os atom. Furthermore, their reported DFT calculations predicted that a lengthening of the N–N bond (by 0.02 Å) should be observed, which also agreed with the observed IR spectrum, where the N–N stretching vibration was downshifted from that of the end-on coordinated N_2.

The 1.120 Å N–N separation calculated for **1e** compares well with the average N–N bond length of 1.11(7) Å determined from 76 experimental structures reported in the Cambridge Structural Database.[30] The bond lengths in complexes **2s–5s** and **2e–5e** can only be compared to those in structures containing P_2, As_2, Sb_2, and Bi_2 coordinated to more than one metal fragment. In complexes containing two metal fragments coordinating in a side-on fashion the average E–E bond lengths are 2.08(5), 2.28(3), 2.678 (only one example[31]) and 2.84(3) Å for P–P, As–As, Sb–Sb, and Bi–Bi, respectively.[30] Despite the fact that these structures involve coordination of the ligand to an extra metal center the distances compare very well to the calculated separations listed in Table 1. In addition, E–E separations in complexes containing two side-on coordinated metal fragments and one or two end-on coordinated metal fragments do not differ significantly from these values either (P_2 coordinated to three metal fragments: 2.07(2) Å; P_2 coordinated to four metal fragments: 2.08(2) Å; As_2 coordinated to four metal fragments: 2.30(2) Å).[30] Thus, surprisingly, it appears that the E–E ligand is not significantly affected by the addition of metal fragments. This statement echoes that of Huttner

Table 1. Selected bond lengths [Å] and angles [°] of neutral $[W(CO)_5(E_2)]$ complexes and free ligands calculated at BP86/TZP. Values at BP86/LANL2DZ(+) are given in parentheses.

		E = N (**1**)	P (**2**)	As (**3**)	Sb (**4**)	Bi (**5**)
free ligand	bond length	1.104 (1.107)	1.935 (1.937)	2.161 (2.124)	2.579 (2.506)	2.728 (2.665)
side-on coordination	bond length E–E	1.129 (1.129)	2.001 (2.007)	2.250 (2.204)	2.674 (2.592)	2.824 (2.752)
	bond lengths E–W	2.474 (2.519)	2.683 (2.695)	2.815 (2.791)	3.020 (2.995)	3.129 (3.064)
	W–C(*trans*)	1.979(1.981)	2.016 (2.021)	2.010 (2.019)	2.005 (2.014)	1.999 (2.010)
	average W–C(*cis*)	2.059 (2.051)	2.065 (2.067)	2.063 (2.066)	2.061 (2.064)	2.059 (2.063)
	bond angle W-E-E	76.81 (77.05)	68.11 (68.14)	66.44 (66.75)	63.72 (64.36)	63.18 (63.32)
end-on coordination	bond length E–E	1.120 (1.121)	1.934 (1.938)	2.161 (2.121)	2.564 (2.496)	2.714 (2.651)
	bond length E–W	2.117 (2.124)	2.434 (2.449)	2.585 (2.556)	2.779 (2.757)	2.913 (2.840)
	W–C(*trans*)	2.019 (2.022)	2.027 (2.029)	2.010 (2.019)	2.002 (2.012)	1.990 (2.003)
	W–C(*cis*)	2.060 (2.062)	2.062 (2.064)	2.061 (2.064)	2.059 (2.062)	2.058 (2.061)

et al.,[2d] who noted that the two extra $Cr(CO)_5$ fragments in $[\{Mo(CO)_2Cp\}_2\{Cr(CO)_5\}_2As_2]$ did not have an obvious influence on the core geometry of $[\{Mo(CO)_2Cp\}_2As_2]$.

Comparison of the calculated values in Table 1 shows that upon side-on coordination the E–E bond becomes increasingly lengthened from that in the uncoordinated molecule along the series **1s**–**5s** (0.022 Å for **1s** to 0.096 Å for **5s**). In the case of the end-on coordinated ligands (**1e**–**5e**), however, only the N–N bond lengthens by 0.013 Å upon metal coordination. The P–P (in **2e**) and As–As (in **3e**) bonds remain unaffected by coordination, while the Sb–Sb (in **4e**) and Bi–Bi (in **5e**) bonds are even shortened (by 0.015 and 0.014 Å, respectively).

The absolute energies, bond dissociation energies (D_e), and zero-point corrected energies (D_0) of the various neutral complexes are given in Table 2. The theoretically predicted trend in the bond dissociation energies is shown in Figure 2. Since the respective BP86/TZP and BP86/LANL2DZ(+) results agree very well, the discussion will compare results in terms of the values obtained at BP86/TZP only.

The theoretically predicted bond dissociation energies indicate that the end-on bonded N_2 ligand in **1e** is much more strongly bound ($D_e = 24.9$ kcal mol^{-1}) than the side-on bonded ligand in **1s** ($D_e = 8.3$ kcal mol^{-1}). In contrast to the N_2 ligand, the heavier ligands P_2–Bi_2 are clearly more strongly bonded in the side-on mode than in the end-on mode. The bond dissociation energies of **2s**–**5s** are much higher ($D_e =$ 37.9 – 39.0 kcal mol^{-1}) than the D_e value of **1s**. Note that the D_e values of the former complexes do not vary very much for the different ligands P_2–Bi_2. In the end-on bonded complexes, **1e-5e**, the phosphorous and arsenic ligands are slightly more strongly bonded than N_2, but Sb_2 and Bi_2 are more weakly bonded than N_2. The different trends in the bond dissociation energies of the side-on and end-on complexes are displayed in Figure 2. What is the explanation for the strong increase in the D_e value from **1s** to **2s**–**5s**, while the change in the bond dissociation energy from **1e** to **2e**–**5e** is much less? In the following discussion we will analyze the metal–ligand interaction to address this question, first looking at the results of the electronic structure analysis and then at the energy decomposition analysis. The quantitative bonding analysis will be carried out in conjunction with the qualitative bonding model which is adapted from the Dewar–Chatt–Duncanson orbital scheme for olefins.[32] The relevant orbital interactions of the side-on complexes are shown in Figure 3. The metal–ligand interactions are discussed in terms of a) σ donation from the in-plane π orbital of the ligand (which has σ symmetry in the complex) to empty orbitals of the metal and b) in-plane π back-donation ($\pi_{\parallel}$) from the filled d(π) AO of the metal into the empty π* orbital of E_2. The ligands with a formal triple bond E≡E may also c) donate from the out-of-plane $\pi_{\perp}$ orbital into the empty d(π) AO of the metal. Finally, there may also be d) out-of-plane back-donation from occupied d(δ) AOs of the metal into the empty π* orbital of

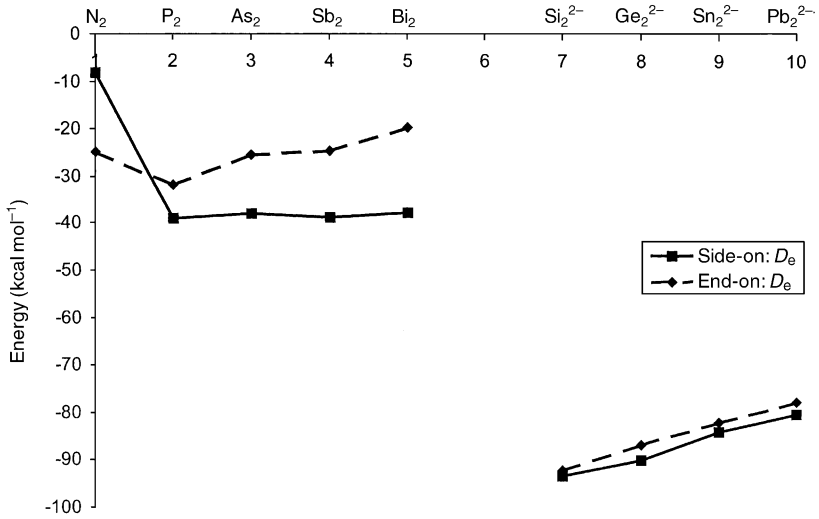

Figure 2. Bond dissociation energies (D_e) of neutral and anionic $[W(CO)_5(E–E)]$ complexes at BP86/TZP in kcal mol^{-1}.

Table 2. Absolute energies, bond dissociation energies D_e, zero-point corrected bond energies D_o of the neutral $[W(CO)_5(E_2)]$ molecules calculated at BP86/TZP. Values at BP86/LANL2DZ(+) are given in parentheses. The energy difference between the end-on and side-on coordination modes ΔE_{coord} is also given.

		E = N (**1**)	P (**2**)	As (**3**)	Sb (**4**)	Bi (**5**)
free ligand	energy (a. u.)	– 0.60644 (– 19.95899)	– 0.31418 (– 13.13543)	– 0.26074 (– 12.50531)	– 0.20031 (– 10.96672)	– 0.18382 (– 10.90759)
side-on coordination	energy (a. u.)	– 3.83795 (– 654.64015)	– 3.59457 (– 647.86455)	– 3.53949 (– 647.23646)	– 3.48060 (– 645.70029)	– 3.46245 (– 645.64391)
	D_e (kcal mol^{-1})	– 8.3 (– 9.2)	– 39.0 (– 39.3)	– 38.0 (– 40.6)	– 38.9 (– 42.1)	– 37.9 (– 43.8)
	D_o (kcal mol^{-1})	– 7.4 (– 8.2)	– 38.0 (– 38.4)	– 37.3 (– 39.9)	– 38.3 (– 41.5)	– 37.4 (43.3)
end-on coordination	energy (a. u.)	– 3.86440 (– 654.66809)	– 3.58314 (– 647.85349)	– 3.51952 (– 647.21758)	– 3.45804 (– 645.67679)	– 3.43349 (– 645.61269)
	D_e (kcal mol^{-1})	– 24.9 (– 26.7)	– 31.8 (32.6)	– 25.4 (– 28.7)	– 24.8 (27.4)	– 19.7 (– 24.2)
	D_o (kcal mol^{-1})	– 23.3 (– 25.2)	– 30.9 (– 31.4)	– 24.8 (– 28.1)	– 24.3 (– 26.9)	– 19.2 (– 23.7)
	ΔE_{coord} (kcal mol^{-1})	– 16.6 (– 17.5)	+ 7.2 (+ 6.9)	+ 12.5 (+ 11.8)	+ 14.2 (+ 14.8)	+ 18.2 (+ 19.6)

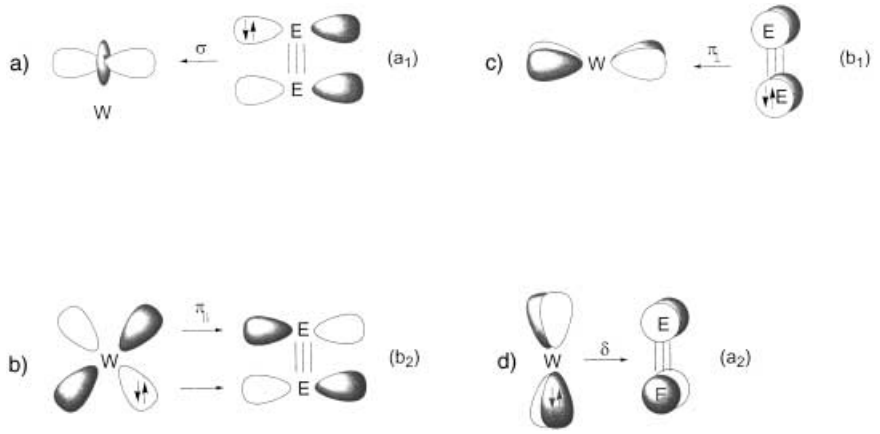

Figure 3. Schematic representation of the bonding models for the side-on coordination of E_2 to $W(CO)_5$, showing donor–acceptor interactions in the a_1(a), a_2 (b), b_1 (c), and b_2 (d) representations.

E_2. Figure 3 shows that the four types of orbital interactions can be distinguished in molecules with C_{2v} symmetry because the orbitals have a_1, b_2, b_1, and a_2 symmetry, respectively.

Results from the natural bond orbital (NBO) analysis, including the E–E and E–W Wiberg bond indices (WBI) and NBO charges on E and W, are listed in Table 3. The WBI values for the E–E bonds in the complexes (**1s**–**5s** and **1e**–**5e**) are lower (between 2.76 for both **1s** and **1e** and 2.13 and 2.61 for **5s** and **5e**, respectively) than the value of 3.0 found in **1**–**5**. This agrees with the previous proposals that the bond order should decrease.[3, 4] Furthermore, there is a significant difference between the dinitrogen complexes **1s**/**1e** and the heavier homologues **2s**/**2e**–**5s**/**5e**. The former species have identical WBI values (2.76), while the side-on complexes **2s**–**5s** have significantly smaller WBI values (2.13–2.25) than the end-on isomers **2e**–**5e** (2.61–2.68). There is very little charge donation from the N_2 $\pi_{\|}$ orbital into the $W(CO)_5$ acceptor orbital in **1s** (0.08 e), but there is significant charge donation from the E_2 $\pi_{\|}$ orbital of the heavier homologues in **2s**–**5s** (0.43–0.61 e). The charge donation from the E_2 $\pi_{\perp}$ orbital in **2s**–**5s** is negligible. At the same time, the charge acceptance of the π* orbital of the N_2 ligand in **1s** (0.17 e) is clearly less than the acceptance of the π* orbital of the E_2 ligands in **2s**–**5s** (0.31–0.36 e), while the π* acceptance of the end-on coordinated ligands in **1e**–**5e** remains small for the heavier ligands as well (0.09–0.12 e). The charge donation from the σ lone pair orbital of the ligands in the latter complexes **1e**–**5e** is much larger (0.26–0.59 e), but its influence on the bond order is small because the σ HOMO of E_2 is only weakly bonding. The WBI values of the E–W bond in the end-on complexes **1e**–**5e** are higher (0.48–0.62) than in the side-on complexes **1s**–**5s** (0.23–0.42), however in the former species there is only one E–W bond, while in the latter there are two.

The significant difference between the dinitrogen complexes **1s**/**1e** and the heavier homologues **2s**/**2e**–**5s**/**5e** also comes to the fore through the calculated total charge exchange between the E_2 ligands and the $W(CO)_5$ fragment. Table 3 shows that the ligands E_2 always carry a positive charge, whereas the partial charge of the N_2 ligand in **1s** (0.02 e) and **1e** (0.03 e) is very small. The partial charges of E_2 in the side-on complexes **2s**–**5s** (0.18–0.40 e) and end-on complexes **2e**–**5e** (0.18–0.28 e) are clearly higher. In summary, the analysis of the electronic structure of **1s**–**5s** and **1e**–**5e** shows significant differences between the dinitrogen species **1s**/**1e** and the heavier homologues **2s**/**2e**–**5s**/**5e**. The WBI bond indices and the charge distribution suggest that the metal–ligand interactions in the side-on coordinated species **2s**–**5s** clearly become stronger than in **1s**, while the differences betwen **1e** and **2e**–**5e** appear to not be very large. From the data it is not obvious, however, why N_2 clearly prefers end-on coordination over side-on coordination. The influence of electrostatic interactions on the metal–ligand bonding in the side-on and end-on complexes also remains unclear. A more detailed insight, that also gives a quantitative estimate of the energy contributions of the covalent and

Table 3. Wiberg bond indices (WBI) and atomic partial charges on E and W (q(E) and q(W)) of neutral $[W(CO)_5(E_2)]$ molecules from NBO analysis calculated at BP86/LANL2DZ(+).

		E =	N (**1**)	P (**2**)	As (**3**)	Sb (**4**)	Bi (**5**)
free ligand	WBI		3.02	3.00	3.00	3.00	3.00
	charge		0	0	0	0	0
side-on coordination	WBI E–E		2.76	2.25	2.21	2.15	2.13
	WBI E–W		0.23	0.42	0.41	0.40	0.38
	q (E)		0.01	0.09	0.12	0.17	0.20
	q (W)		−0.59	−0.79	−0.80	−0.82	−0.80
	no. electrons donated from E–E $\pi_{\|}$ orbital		0.08	0.43	0.48	0.57	0.61
	no. electrons donated from E–E $\pi_{\perp}$ orbital		0.01	0.05	0.05	0.06	0.07
	no. of electrons accepted into E–E π* orbital		0.17	0.36	0.35	0.33	0.31
end-on coordination	WBI E–E		2.76	2.68	2.66	2.66	2.61
	WBI E–W		0.50, 0.16	0.62, 0.15	0.57, 0.15	0.53, 0.14	0.48, 0.16
	q(E coordinated, E terminal)		−0.05, 0.08	0.12, 0.06	0.13, 0.08	0.18, 0.09	0.17, 0.11
	q(W)		−0.57	−0.83	−0.83	−0.83	−0.81
	no. electrons donated from E lone pair orbital		0.26	0.41	0.34	0.59	0.25
	no. of electrons accepted into E–E π* orbital		0.12	0.13	0.12	0.11	0.09

electrostatic interactions, is given by the energy decomposition analysis (EDA), whose results are presented in the following section.

Table 4 gives the EDA results for the side-on complexes **1s**–**5s** and the end-on complexes **1e**–**5e**. It becomes obvious that the calculated metal–ligand interaction energies ΔE_{int} show the same trend as the bond dissociation energies D_e. It follows that the different bonding behavior of the E_2 ligands is indeed caused by the intrinsic bonding interactions and not by relaxation effects. The trends of the different energy terms of the metal–ligand interaction energies are displayed in Figure 4 and Figure 5.

We begin with the side-on coordinated complexes **1s**–**5s**. Table 4 shows that the $(CO)_5W-N_2$ interactions in **1s** are approximately two thirds covalent ($\Delta E_{orb} = 66.0\,\%$) and one third electrostatic ($\Delta E_{elstat} = 34.0\,\%$). The bonding in the heavier homologues **2s**–**5s** has a uniformly higher degree of electrostatic character ($\Delta E_{elstat} = 46.6 - 48.4\,\%$) which suggests that the bonding in the latter compounds is approximately half covalent and half electrostatic. The breakdown of the ΔE_{orb} term into orbital con-

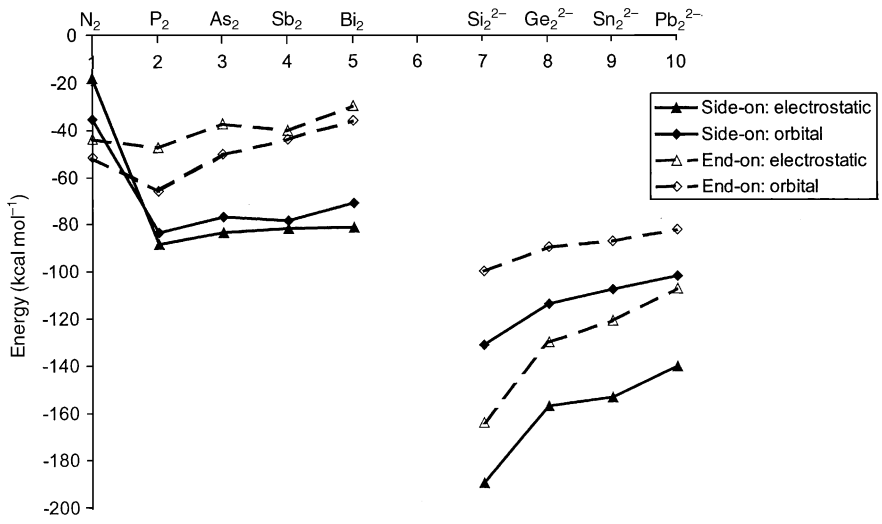

Figure 4. Comparison of electrostatic and orbital interactions for $W(CO)_5$ complexes containing neutral and anionic E_2 ligands coordinated in side-on and end-on modes.

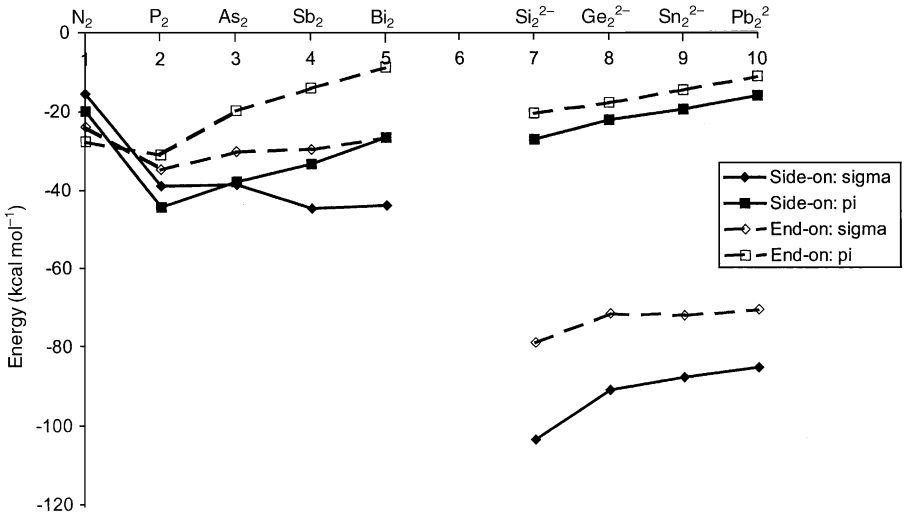

Figure 5. Comparison of σ and π interactions for $W(CO)_5$ complexes containing neutral and anionic E_2 ligands coordinated in side-on and end-on modes.

Table 4. Energy decomposition analysis of the neutral $[W(CO)_5(E_2)]$ molecules calculated at BP86/TZP. The symmetry point group for the side-on coordination mode is C_{2v} and C_{4v} for the end-on coordination mode. All values are in kcal mol^{-1}.

	E =	N (**1**)	P (**2**)	As (**3**)	Sb (**4**)	Bi (**5**)
side-on	ΔE_{int}	– 10.1	– 43.7	– 43.1	– 44.0	– 42.4
coordination	ΔE_{Pauli}	43.5	128.2	117.4	116.3	110.0
	ΔE_{Elstat}	– 18.2 (33.9 %)	– 88.6 (51.5 %)	– 83.7 (52.1 %)	– 81.9 (51.0 %)	– 81.3 (53.3 %)
	ΔE_{Orb}	– 35.4 (66.0 %)	– 83.4 (48.4 %)	– 76.8 (47.8 %)	– 78.4 (48.9 %)	– 71.1 (46.6 %)
	a_1 (σ)	– 14.4 (40.5 %)	– 35.3 (42.3 %)	– 35.8 (46.5 %)	– 42.4 (54.2 %)	– 42.4 (59.7 %)
	a_2 (δ)	– 1.1 (3.1 %)	– 3.6 (4.4 %)	– 3.0 (3.9 %)	– 2.4 (3.1 %)	– 1.8 (2.5 %)
	b_1 ($\pi_\perp$)	– 1.5 (4.3 %)	– 4.9 (5.9 %)	– 3.7 (4.8 %)	– 3.6 (4.6 %)	– 3.1 (4.4 %)
	b_2 ($\pi_\parallel$)	– 18.4 (52.0 %)	– 39.5 (47.4 %)	– 34.4 (44.8 %)	– 29.9 (38.1 %)	– 23.8 (33.5 %)
end-on	ΔE_{int}	– 27.1	– 33.8	– 26.8	– 25.9	– 20.4
coordination	ΔE_{Pauli}	68.2	79.5	61.1	58.6	45.9
	ΔE_{Elstat}	– 43.8 (45.9 %)	– 47.5 (41.8 %)	– 37.6 (42.7 %)	– 40.5 (47.9 %)	– 30.2 (45.5 %)
	ΔE_{Orb}	– 51.4 (54.0 %)	– 65.9 (58.1 %)	– 50.3 (57.2 %)	– 44.0 (52.0 %)	– 36.1 (54.4 %)
	a_1 (σ)	– 23.8 (46.3 %)	– 34.7 (52.8 %)	– 30.2 (60.1 %)	– 29.8 (67.7 %)	– 27.0 (74.7 %)
	a_2	0	0	0	0	0
	b_1	– 0.1 (0.1 %)	– 0.2 (0.2 %)	– 0.1 (0.1 %)	0.0 (0.0 %)	0.0 (0.1 %)
	b_2	0.0 (0.1 %)	– 0.2 (0.2 %)	– 0.1 (0.2 %)	0.0 (0.1 %)	0.0 (0.1 %)
	e_1 (π)	– 27.5 (53.5 %)	– 30.8 (46.8 %)	– 19.9 (39.6 %)	– 14.2 (32.3 %)	– 9.1 (25.2 %)

tributions of different symmetry reveals that, in the dinitrogen complex **1s**, the π interactions are stronger than the σ interactions. The $a_1(\sigma)$ interactions increase continuously from **1s** (40.5%) to **5s** (59.7%). Note that the charge donation of the ligand out-of-plane $\pi_\perp$ orbital (b_1 orbital in the complex) and the out-of-plane back-donation from occupied d(δ) AOs of the metal (a_2 orbital in the complex) contribute very little to the covalent bonding in all complexes (Table 4).

The largest difference between the EDA results of the end-on bonded dinitrogen complex **1e** and the side-on bonded isomer **1s** is the significantly higher degree of electrostatic attraction in the former species ($\Delta E_{elstat} = 46.0\%$) as compared to the latter ($\Delta E_{elstat} = 34.0\%$). This is in agreement with the conclusion of Sakaki et al.,[33] which they drew from their ab initio study of $[RhCl(PH_3)_2(N_2)]$. The authors suggested that one of the reasons for the greater stability of the end-on coordination mode is that it receives greater stabilization from the electrostatic interactions. While the end-on bonded dinitrogen complex **1e** has a *higher* degree of electrostatic bonding than the side-on bonded isomer **1s**, the bonding in the heavier homologues **2e**–**5e** exhibits *less* electrostatic character than in **2s**–**5s**. The EDA results in Table 4 indicate that the relative contributions of covalent and electrostatic bonding in **1e** are not very different from the heavier homologues **2e**–**5e**. The σ contribution to the ΔE_{orb} term increases smoothly from **1e** (46.3%) to **5e** (74.7%) and thus, it exhibits the same trend as for the side-on bonded species. The increase in the σ contribution to ΔE_{orb} in the end-on and side-on complexes is displayed in Figure 5. The dominant influence of the ΔE_{elstat} term becomes visible from Figure 4, which shows the trends of the electrostatic and covalent contributions to the metal–ligand interactions in the end-on and side-on complexes. The curves of the ΔE_{elstat} term of the two isomeric forms cross from nitrogen to phosphorus, while the curves of the ΔE_{elstat} term change less. *The most important conclusion that can be drawn from the energy decomposition analysis is as follows: The preference of the heavier homologues, P_2–Bi_2, for binding in a side-on mode over the end-on mode in the complexes $(CO)_5W$–E_2, which is opposite to the behavior of N_2, comes mainly from the much stronger electrostatic attraction in **2s**–**5s**.*

It is interesting to compare the results of the NBO analysis (Table 3) with the results of the EDA calculations (Table 4). Some trends in the charge analysis are in agreement with the calculated energy contributions to the bonding interactions. For example, the theoretically predicted σ donation in the side-on bonded complex **1s**, which comes from the occupied π orbital[32] of N_2 (0.08 e), is less than the calculated acceptor charge of the π* orbital (0.17 e), which is in agreement with the larger energy contribution to ΔE_{orb} by the b_2 orbitals than the a_1 orbitals. The calculated charge donation from the π orbital and the charged acceptance of the π* orbital is higher for the heavier E_2 ligands in **2s**–**5s** than in **1s** (Table 3) which agrees with the larger contributions by the a_1 and b_2 orbitals to ΔE_{orb} (Table 4). The small amount of charge donation from the $\pi_\perp$ orbitals in **1e**–**5e** are also in agreement with the low energy contributions of the b_1 orbitals. However, the charge acceptance of the π* orbitals calculated for the end-on complexes **1e**–**5e** is very small (0.09–0.13 e), which is at variance with the substantial energy contribution by the e_1 orbital, which is particularly large in **1e** and **2e** (Table 4). In addition, the small differences between the calculated π* acceptor charges do not agree with the substantially different energy contributions by the e_1 orbitals. Note that the electronic charge is donated into the π* orbitals of E_2, which are built from the $n(p_\pi)$ AOs, where n changes from 2 (E = N) to 6 (E = Bi). The energy levels of the orbitals are very different but the energetic effect of the charge donation is not apparaent from the occupation number. It is important to recognize that although charge partitioning methods are useful for gaining insight into the electronic structure of a molecule, it is difficult to obtain information about the energy contributions to the interatomic interactions from a charge analysis.

The lengthening of the E–E distance upon side-on coordination in the complexes **1s**–**5s** can be explained by the metal–E_2 orbital interactions that weaken the E–E bonding through charge donation from the E_2 π bonding orbital and charge acceptance into the π* orbital. This model is quantitatively supported by the calculated energy values of the a_1 and b_2 orbital contributions to the ΔE_{elstat} term that are given in Table 4. But what about the E–E distance in the end-on coordinated complexes **1e**–**5e**, which is only slightly longer or even shorter than in the free ligands? Sakaki et al.[33] also noted in their theoretical study of $[RhCl(PH_3)N_2]$ that the N_2 separation did not lengthen as much as expected upon coordination and ascribed this to attractive electrostatic interactions between the two N atoms as a result of the opposite charge of the nitrogen atoms in the complex. In our study the N–N bond length in **1e** is also not lengthened as much as in **1s**. However, **2e** to **5e** do not exhibit a charge difference, and yet show less lengthening or even shortening of the bond upon end-on coordination, as described above. To understand this effect and in order to gain insight into the change in the E–E bonding situation between the free ligand E_2 and the end-on coordinated complexes we analyzed the E–E bonding between $W(CO)_5E$ and E and compared it to the bonding in E–E. The results of this analysis are shown in Table 5.

The values in Table 5 shows that the attractive interactions in E_2 have a significant electrostatic character. The electrostatic contributions to the E–E bonding in the free ligands E_2 increases from 30.0% in N_2 to 57.6% in Bi_2. Thus, there is a significant electrostatic attraction in E_2, to the extent that it becomes the largest contributor to the bonding interaction in Sb_2 and Bi_2. This result seems surprising since standard textbook knowledge teaches that unpolar bonds are purely covalent. However, a theoretical analysis by Spackman and Maslen of the interatomic electrostatic interactions between two spherical atoms showed already that the electrostatic attraction in homoatomic species E_2 is larger than the total bonding energy with the notable exception of H_2.[34] The results in Table 5 are in agreement with the data of Spackman and Maslen, with the absolute values of the ΔE_{elstat} term always being larger than ΔE_{int}. Another surprising result, which contradicts common knowledge, is the relative strength of the π bonding contribution in E_2. It is well known that

Table 5. Energy decomposition analysis of the neutral $[(W(CO)_5E)-E]$ and E–E molecules calculated at BP86/TZP. The symmetry point group is C_{4v} for the end-on coordination mode. All values are in kcal mol^{-1}.

	E =	N (**1**)	P (**2**)	As (**3**)	Sb (**4**)	Bi (**5**)
free ligand	ΔE_{int}	−237.8	−113.9	−88.2	−62.0	−55.5
	ΔE_{Pauli}	794.8	298.8	247.5	182.5	168.5
	ΔE_{Elstat}	−310.6 (30.1%)	−176.8 (42.8%)	−162.4 (48.4%)	−134.1 (54.8%)	−129.2 (57.7%)
	ΔE_{Orb}	−721.9 (69.9%)	−235.9 (57.2%)	−173.3 (51.6%)	−110.5 (45.2%)	−94.8 (42.3%)
	a_1 (σ)	−474.6 (65.7%)	−141.5 (60.0%)	−106.8 (61.6%)	−71.3 (64.5%)	−62.2 (65.6%)
	a_2	0	0	0	0	0
	b_1	0	0	0	0	0
	b_2	0	0	0	0	0
	e_1 (π)	−247.3 (34.3%)	−94.4 (40.0%)	−66.4 (38.4%)	−39.2 (35.5%)	−32.6 (34.4%)
end-on coordination	ΔE_{int}	−241.2	−130.0	−101.0	−75.5	−65.1
	ΔE_{Pauli}	716.3	257.8	208.3	154.8	138.6
	ΔE_{Elstat}	−274.1 (28.6%)	−143.5 (37.0%)	−128.6 (41.6%)	−107.7 (46.7%)	−98.4 (48.3%)
	ΔE_{Orb}	−683.4 (71.4%)	−244.3 (63.0%)	−180.7 (58.4%)	−122.7 (53.3%)	−105.3 (51.7%)
	a_1 (σ)	−437.3 (63.9%)	−139.8 (57.2%)	−107.7 (59.6%)	−76.6 (62.4%)	−66.8 (63.4%)
	a_2	0	0	0	0	0
	b_1	−0.2 (0.1%)	0.0 (0.0%)	0.0 (0.0%)	0.0 (0.0%)	0.0 (0.0%)
	b_2	−0.1 (0.0%)	−0.1 (0.1%)	0.0 (0.0%)	0.0 (0.0%)	0.0 (0.0%)
	e_1 (π)	−245.8 (36.0%)	−104.5 (42.7%)	−73.0 (40.4%)	−46.0 (37.6%)	−38.4 (36.6%)

molecules containing π bonds between elements of the first octal row are stable, while unsaturated homologues of heavier elements are difficult to produce. This is usually explained by the weakness of the π bond between the heavier elements. Table 5 shows that the percentage contribution of the π bonds of P_2–Bi_2 (34.3–40.0%) to the covalent bonding is *higher* than in N_2 (34.2%). The difficulty in preparing stable compounds with multiple bonds of heavier elements is not caused by the intrinsically weak π bonding but by the comparatively high energy gain by the latter molecules in reactions, which leads to molecules with single bonds.

Here our interest focuses on the *change* in the E–E interactions upon coordination with $W(CO)_5$. Table 5 shows rather uniform alterations in **1e**–**5e**. The interaction energy ΔE_{int} becomes continuously higher, which means that, in the complexes, there is stronger E–E interatomic attraction. Note that the increase in the ΔE_{int} values does not correlate with the change in the E–E bond lengths (Table 1). In the complexes, the N–N distance becomes longer than in free N_2, the P–P and As–As distances remain nearly the same, while the Sb–Sb and Bi–Bi bonds become longer than in free E_2. Table 5 shows that the E–E bonds in the complexes always have a higher covalent character (51.6–71.3%) than in free E_2 (42.3–69.9%). The covalent bonding in **1e**–**5e** has a slightly higher contribution from π bonding (36.0–42.7%) than in E_2 (34.2–40.0%).

In their study of end-on coordinated $[RhCl(PH_3)N_2]$ Sakaki et al.[33] found that the N_2 separation did not lengthen as much as expected upon coordination and ascribed this to attractive electrostatic interactions, since the charge on the coordinated N atom was negative, while the other N atom was positive. Opposite charges at the nitrogen atoms are also calculated for **1e** (Table 2). However, the EDA results show that the electrostatic attraction between the nitrogen atoms of **1e** is weaker than in N_2 (Table 5). It has already been pointed out by us that atomic partial charges are not a reliable probe for electrostatic interactions because the electron density distribution of an atom in a molecule is in most cases anisotropic.[35]

Anionic complexes: The complexes containing anionic group-14 E_2 ligands coordinated in side-on and end-on modes have similar geometries to their neutral Group 15 counterparts. Table 6 lists selected bond lengths and angles for complexes **7s**–**10s** and **7e**–**10e**, as well as the free anions **7**–**10**.

No comparable structures have been reported for complexes containing the anionic ligands, other than the star-type

Table 6. Selected bond lengths [Å] and angles [°] of anionic $[W(CO)_5(E_2)]^{2-}$ complexes and free ligands calculated at BP86/TZP. Values at BP86/LANL2DZ(+) are given in parentheses.

		E =	Si^- (**7**)	Ge^- (**8**)	Sn^- (**9**)	Pb^- (**10**)
free ligand	bond length		2.270 (2.204)	2.357 (2.329)	2.717 (2.701)	2.886 (2.794)
side-on coordination	bond length E–E		2.227 (2.239)	2.396 (2.371)	2.769 (2.743)	2.908 (2.838)
	bond lengths E–W		2.886 (2.903)	3.036 (2.995)	3.218 (3.197)	3.346 (3.298)
	W–C(*trans*)		1.973 (1.979)	1.964 (1.975)	1.961 (1.968)	1.957 (1.964)
	average W–C(*cis*)		2.052 (2.054)	2.051 (2.054)	2.052 (2.052)	2.051 (2.053)
	bond angle W-E-E		67.31 (67.32)	66.76 (66.68)	64.51 (64.59)	64.24 (64.51)
end-on coordination	bond length E–E		2.143 (2.154)	2.286 (2.273)	2.647 (2.631)	2.782 (2.719)
	bond length E–W		2.716 (2.719)	2.836 (2.800)	3.001 (2.983)	3.130 (3.077)
	W–C(*trans*)		1.982 (1.985)	1.973 (1.980)	1.970 (1.976)	1.965 (1.972)
	W–C(*cis*)		2.045 (2.045)	2.044 (2.045)	2.044 (2.045)	2.043 (2.045)

complex, $[\{W(CO)_5\}_4Pb_2]^{2-}$ (Pb–Pb bond length 2.806(8) Å).[5] The experimental Pb–Pb bond length in $[\{W(CO)_5\}_4Pb_2]^{2-}$ is in between the values calculated for **10s** and **10e**. This suggests that, since coordination of a single metal fragment in side-on coordination mode results in a lengthening of the E–E bond, while end-on coordination has the opposite effect, the presence of metal fragments in both side-on and end-on coordination modes in $[\{W(CO)_5\}_4Pb_2]^{2-}$ results in an intermediate length. The E–E bond lengths follow a similar trend to those in the complexes with neutral ligands—side-on coordination of the complexes results in a lengthening of the E–E bond relative to the value in the free dianion, whereas in the end-on coordination mode the E–E bond is shortened.

The absolute energies, dissociation energies (D_e) and zero-point corrected energies (D_0) of the various anionic complexes are listed in Table 7, with the bond energies in comparison to those of the neutral ligands graphically represented in Figure 2. The results show that the anionic ligands are far more strongly bonded than in the case of the neutral ligands, irrespective of whether the coordination is side-on or end-on ($D_e = 78.0 - 93.5$ kcal mol^{-1}). As with the corresponding neutral complexes the E_2 ligands are more strongly bonded in the side-on coordination mode than the end-on mode (difference in $D_e = 1.2 - 3.3$ kcal mol^{-1}), although the difference in energy of less than 3.3 kcal mol^{-1} indicates that the preference for side-on coordination is not as great as for the neutral ligands. We will again analyze these results by means of the electronic structure analysis and energy decomposition analysis.

A list of E–E and E–W Wiberg bond indices (WBI) and the natural bond orbital (NBO) charges on E and W are given in Table 8.

As with the neutral complexes the WBI values of the E–E bonds in **7s–10s** and **7e–10e** are lower than the value of 3.0 found for **7–10**. The WBI values for **7s–10s** are lower than for the corresponding neutral complexes (**1s–5s**), and indicate that the anionic ligands have double bond character in the side-on coordinated complexes. These low values can be correlated to the significant amount of charge donation from the E_2 in-plane $\pi_{\parallel}$-orbital,[32] which is substantially greater (0.83–0.93 e) than in **1s–5s**. The donation from the $\pi_{\perp}$ orbital of the ligands is always small in the latter complexes but larger than in the neutral species. Note that the charge acceptance by the π^* orbital (0.11–0.12) is less than for **1s–5s**. In the end-on coordinated complexes **7e–10e**, however, the WBI values (2.59–2.79) are very similar to the values found for **1e–5e**. The charge donation from the σ lone pair orbital (0.92–1.27 e) is significantly larger than in **1e–5e**, but as with the neutral complexes the σ HOMO of E_2 is weakly bonding, thus its influence on the bond order is small. The E–W WBI values of **7s–10s** (0.20–0.23) and **7e–10e** (0.29–0.37) are lower than those for the neutral ligands. The NBO charges show that much of the charge is delocalized from the previously anionic

Table 7. Absolute energies, bond dissociation energies D_e, zero-point corrected bond energies D_o of the anionic $[W(CO)_5(E_2)]^{2-}$ molecules calculated at BP86/TZP. Values at BP86/LANL2DZ(+) are given in parentheses. The energy difference between the end-on and side-on coordination modes ΔE_{coord} is also given.

		E = Si$^-$ (**7**)	Ge$^-$ (**8**)	Sn$^-$ (**9**)	Pb$^-$ (**10**)
free ligand	energy (a. u.)	−0.16614 (−7.68339)	−0.15573 (−7.62374)	−0.13629 (−6.81074)	−0.11724 (−6.92549)
side-on coordination	energy (a. u.)	−3.54021 (−642.53392)	−3.52454 (−642.46653)	−3.49561 (−641.64077)	−3.47071 (−641.75222)
	D_e (kcal mol^{-1})	−93.5 (−101.6)	−90.2(−96.7)	−84.3 (−88.7)	−80.6 (−86.6)
	D_o (kcal mol^{-1})	−93.4 (−101.5)	−90.4 (−96.9)	−84.5 (−89.0)	−80.2 (−86.2)
end-on coordination	energy (a. u.)	−3.53831 (−642.52956)	−3.51934 (−642.46116)	−3.49260 (−641.63798)	−3.46649 (−641.74760)
	D_e (kcal mol^{-1})	−92.3 (−98.8)	−87.0 (−93.4)	−82.4 (−87.0)	−78.0 (−83.8)
	D_o (kcal mol^{-1})	−92.1 (−98.6)	−87.0 (−93.4)	−82.5 (−87.1)	−78.2 (−83.9)
	ΔE_{coord} (kcal mol^{-1})	+1.2 (+2.7)	+3.3 (+3.4)	+1.9 (+1.8)	+2.6 (+2.9)

Table 8. Wiberg bond indices (WBI) and atomic partial charges on E and W (q(E) and q(W)) of anionic $[W(CO)_5(E_2)]^{2-}$ molecules from NBO analysis calculated at BP86/LANL2DZ(+).

		E = Si$^-$ (**7**)	Ge$^-$ (**8**)	Sn$^-$ (**9**)	Pb$^-$ (**10**)
free ligand	WBI	3.02	3.01	3.00	3.01
	charge	−1	−1	−1	−1
side-on coordination	WBI E–E	2.03	2.00	1.97	2.00
	WBI E–W	0.23	0.22	0.22	0.20
	q (E)	−0.42	−0.43	−0.42	−0.44
	q (W)	−0.69	−0.67	−0.65	−0.6
	no. electrons donated from E–E $\pi_{\parallel}$ orbital	0.83	0.86	0.91	0.93
	no. electrons donated from E–E $\pi_{\perp}$ orbital	0.17	0.15	0.15	0.13
	no. of electrons accepted into E–E π^* orbital	0.13	0.12	0.12	0.11
end-on coordination	WBI E–E	2.79	2.71	2.68	2.59
	WBI E–W	0.37, 0.05	0.34, 0.07	0.32, 0.08	0.29, 0.10
	q(E coordinated, E terminal)	−0.41, −0.60	−0.38, −0.63	−0.29, −0.70	−0.29, −0.71
	q(W)	−0.71	−0.68	−0.67	−0.64
	no. electrons donated from E lone pair orbital	0.92	1.04	1.11	1.27
	no. of electrons accepted into E–E π^* orbital	0.16	0.24	0.25	0.32

E_2 ligand, with complexes **7s**–**10s** exhibiting very similar charges (−0.42 to −0.44). In complexes **7e**–**10e** the NBO charge on the coordinated atom decreases from −0.41 to −0.29 along the series, with a concomitant increase in the NBO charge on the other E atom (from −0.61 to −0.71).

The energy decomposition analysis results, shown in Table 9 and Figure 4 and Figure 5, give a clearer picture of the covalent and electrostatic interactions involved in the formation of the anionic complexes. Note that the relative strength of the ΔE_{int} values also predicts that the side-one bonded complexes are slightly more stable than the end-on bonded isomers.

First we will look at the results for the side-on coordinated complexes **7s**–**10s**. As might be expected the electrostatic interactions between the anionic E_2 ligand and the metal fragment play a much greater role than in the neutral complexes ($\Delta E_{elstat} = -140.5$ to -189.8 kcal mol^{-1}), so that despite an increase in the orbital interactions ($\Delta E_{orb} = -102.0$ to -131.4 kcal mol^{-1}) the interactions are ~60% electrostatic in character. The orbital contributions of different symmetries to the ΔE_{orb} term shows that the σ bonding is significantly larger (78.0–83.1%) than in the neutral complexes. The ligand-out-of-plane $\pi_\perp$ orbital (b_1 orbital in the complex) also contributes more to the covalent bonding. This is in agreement with the slightly larger charge donation of the $\pi_\perp$ orbital given by the NBO analysis. The energy contribution of the out-of-plane back-donation from occupied d(δ) AOs of the metal (a_2 orbital in the complex) remains small, however.

In the end-on coordinated complexes, **7e**–**10e**, the electrostatic interactions also play a larger role than in the neutral complexes, so that the orbital interactions are about 60% electrostatic. This value is similar to that for **7s**–**10s**, despite both electrostatic and orbital interactions being weaker in **7e**–**10e**. The σ bonding interactions, given by the breakdown of the ΔE_{orb} term, are larger than in the neutral complexes, contributing about 80% of the orbital interactions.

The ΔE_{elstat} and ΔE_{orb} terms are more negative for **7s**–**10s** when compared with **7e**–**10e**. The stabilization of the side-on coordination mode with respect to the end-on mode can thus be ascribed to both the electrostatic and orbital energy terms. This is different to the neutral complexes, where the ΔE_{elstat} term could be identified as responsible for the lower energy of **2s**–**5s**. The Pauli repulsion, on the other hand, is substantially larger for **7s**–**10s** (difference between ΔE_{orb} terms = 47.2–56.7 kcal mol^{-1}), with the result that the overall energy difference between the side-on and end-on coordinated complexes is small, but nevertheless favors the side-on coordination mode. The conclusion is that the slightly lower energy of the side-on bonded complexes **7s**–**10s** can not be ascribed to a particular energy component.

If we now return to the NBO analysis we can see that the large charge donation from the $\pi_\parallel$ orbitals predicted for **7s**–**10s** (larger than for **1s**–**5s**) agrees with the large σ bonding term calculated in the EDA results (also larger than for **1s**–**5s**). The same is true for the large amount of charge donation from the σ lone pair orbital in **7e**–**10e**, which agrees with the large σ bonding contribution predicted by the EDA. The small contribution by the π-bonding in **7s**–**10s** and **7e**–**10e** to the orbital interactions is echoed by the small amount of charge acceptance by the E_2 π* orbital. However, the EDA results show that the strength of both the σ and π bonding decreases along the series **7s**–**10s** and **7e**–**10e**, whereas the NBO analysis suggests that the reverse is true, for all except the charge acceptance into the π* orbitals of **7s**–**10s**.

Since the E–E bonds in **7e**–**10e** showed an even greater shortening upon end-on coordination than their neutral counterparts the bonding was analysed as before by using the $W(CO)_5E^-$ and E^- as fragments in the energy decomposition analysis (Table 10). The results show that the bonding in the complexes (52.5–66.3%) has a slightly greater covalent character than in the free anionic molecules (45.7–66.5%). The π-bonding contribution to the covalent bonding is slightly larger (28.9–34.1%) than in the free molecules (28.0–29.7%), but is sufficient to explain the shortening in the bond.

Conclusion

The calculation of $W(CO)_5$ with neutral diatomic ligands N_2, P_2, As_2, Sb_2, and Bi_2 and anionic ligands Si_2^{2-}, Ge_2^{2-}, Sn_2^{2-},

Table 9. Energy decomposition analysis of the anionic $[W(CO)_5(E_2)]^{2-}$ molecules calculated at BP86/TZP. The symmetry point group for the side-on coordination mode is C_{2v} and C_{4v} for the end-on coordination mode. All values are in kcal mol^{-1}.

		E =	Si^- (**7**)	Ge^- (**8**)	Sn^- (**9**)	Pb^- (**10**)
side-on	ΔE_{int}		−99.5	−95.4	−89.3	−86.0
coordination	ΔE_{Pauli}		221.7	175.8	172.0	156.5
	ΔE_{Elstat}		−189.8 (59.1%)	−157.3 (58.0%)	−153.3 (58.7%)	−140.5 (57.9%)
	ΔE_{Orb}		−131.4 (40.9%)	−113.9 (42.0%)	−108.0 (41.3%)	−102.0 (42.1%)
	a_1 (σ)		−102.5 (78.0%)	−90.0 (79.0%)	−87.1 (80.6%)	−84.8 (83.1)
	a_2 (δ)		−1.5 (1.1%)	−1.2 (1.1%)	−1.1 (1.0%)	−0.9 (0.9%)
	b_1 ($\pi_\perp$)		−12.3 (9.4%)	−9.4 (8.3%)	−8.4 (7.8%)	−6.5 (6.3%)
	b_2 ($\pi_\parallel$)		−15.1 (11.5%)	−13.2 (11.6%)	−11.4 (10.6%)	−9.9 (9.7%)
end-on	ΔE_{int}		−99.1	−91.3	−86.3	−82.2
coordination	ΔE_{Pauli}		165.0	128.6	122.0	107.6
	ΔE_{Elstat}		−164.1 (62.1%)	−130.1 (59.2%)	−121.2 (58.2%)	−107.5 (56.6%)
	ΔE_{Orb}		−100.0 (37.9%)	−89.8 (40.8%)	−87.2 (41.8%)	−82.3 (43.4%)
	a_1 (σ)		−79.0 (79.0%)	−71.6 (79.7%)	−72.3 (82.9%)	−70.7 (85.9%)
	a_2		−0.3 (0.3%)	−0.2 (0.2%)	−0.2 (0.2%)	−0.1 (0.2%)
	b_1		−0.8 (0.8%)	−0.5 (0.6%)	−0.5 (0.6%)	−0.5 (0.6%)
	b_2		−0.7 (0.7%)	−0.7 (0.8%)	−0.4 (0.5%)	−0.3 (0.4%)
	e_1 (π)		−19.2 (19.2%)	−16.8 (18.7%)	−13.8 (15.8%)	−10.6 (12.9%)

Table 10. Energy decomposition analysis of the anionic $[(W(CO)_5E)-E]^{2-}$ and $[E-E]^{2-}$ molecules calculated at BP86/TZP. The symmetry point group C_{4v}. All values are in kcal mol^{-1}.

		E = Si$^-$ (**7**)	Ge$^-$ (**8**)	Sn$^-$ (**9**)	Pb$^-$ (**10**)
free ligand	ΔE_{int}	4.6	5.3	13.4	19.0
	ΔE_{Pauli}	227.4	216.9	195.4	188.5
	ΔE_{Elstat}	−74.6 (33.5%)	−84.5 (40.0%)	−89.1 (49.0%)	−91.9 (54.2%)
	ΔE_{Orb}	−148.2 (66.5%)	−127.0 (60.0%)	−92.8 (51.0%)	−77.6 (45.8%)
	A1 (σ)	−106.6 (71.9%)	−89.5 (70.5%)	−65.9 (71.0%)	−54.5 (70.2%)
	A2	0	0	0	0
	B1	0	0	0	0
	B2	0	0	0	0
	E1 (π)	−41.6 (28.1%)	−37.5 (29.5%)	−27.0 (29.0%)	−23.1 (29.8%)
end-on coordination	ΔE_{int}	−36.5	−30.9	−19.2	−12.0
	ΔE_{Pauli}	203.6	194.9	175.0	162.9
	ΔE_{Elstat}	−80.8 (33.6%)	−85.4 (37.8%)	−89.7 (46.2%)	−83.1 (47.5%)
	ΔE_{Orb}	−159.4 (66.4%)	−140.4 (62.2%)	−104.5 (53.8%)	−91.8 (52.5%)
	A1 (σ)	−104.9 (65.8%)	−93.9 (66.9%)	−72.3 (69.2%)	−65.3 (71.1%)
	A2	−0.1 (0.1%)	0.0 (0.0%)	0.0 (0.0%)	0.0 (0.0%)
	B1	−0.2 (0.1%)	−0.1 (0.1%)	−0.1 (0.1%)	−0.1 (0.1%)
	B2	−0.2 (0.1%)	−0.2 (0.1%)	−0.1 (0.1%)	−0.1 (0.1%)
	E1 (π)	−54.1 (33.9%)	−46.2 (32.9%)	−31.9 (30.6%)	−26.4 (28.7%)

and Pb_2^{2-} coordinated in both side-on and end-on modes using density functional methods was presented in this paper. The calculations showed that the neutral ligands prefer side-on coordination modes, with the exception of N_2, which coordinates preferentially in end-on mode, as indicated in the literature. The anionic ligands show only a slight preference for side-on coordination. Energy decomposition analysis results indicate that the electrostatic interactions between the ligand and the metal fragment play the decisive role in deciding the coordination mode in the neutral complexes. In the case of the N_2 complex it is the weakness of the electrostatic interactions in the side-on coordination mode that destabilizes it relative to the end-on mode. For all other ligands the electrostatic interactions between the metal and ligand in side-on coordination mode are stronger than for end-on. The electrostatic interactions between the neutral ligands **2s**–**5s** and the metal fragments in end-on mode are particularly weak, resulting in the strong preference for side-on coordination. The anionic ligands, not surprisingly, exhibit much greater electrostatic interactions with the metal fragments in both the side-on and end-on coordination modes, however the difference in stabilization is smaller than for the neutral ligands, with the effect that the preference for the side-on coordination mode is not as pronounced.

This work thus shows that it should, in principle, be possible to obtain complexes of P_2, As_2, Sb_2, Bi_2, Si_2^{2-}, Ge_2^{2-}, Sn_2^{2-}, and Pb_2^{2-} coordinated to a single metal fragment in a side-on coordination mode since the theoretically predicted binding energies are rather high. The fact that none have been structurally characterized suggests that coordination to 2 or more metal fragments is even more stable. Calculations to confirm this are currently in progress in our laboratory.

NBO and EDA results show that the bonding situation in the complexes is similar for the neutral and anionic ligands. The E–E WBI decreases from 3 in the free ligand to between 2 and 2.8 in all complexes. The NBO analysis shows that in the side-on coordination mode charge donation from the neutral ligands is lower than in the anionic ligands, thus the E–E WBI values are higher. The E–E WBI values are less affected by the amount of charge donation when the E_2 ligands are coordinated in an end-on mode, with the WBI values being similar for all complexes. The E–E bond lengths in the end-on coordinated complexes, **2e**–**10e**, were found to be shortened relative to the free ligands. This was ascribed to the π-bonding involved in the E–E bonding strengthening upon coordination.

We are currently extending this work to look at complexes where the E_2 ligands coordinate to more than one metal fragment.

Acknowledgement

This work was supported by the Deutsche Forschungsgemeinschaft and by the Fonds der Chemischen Industrie. C. Esterhuysen thanks the Alexander von Humboldt Foundation for a research fellowship. Excellent service by the Hochschulrechenzentrum of the Philipps-Universität Marburg is gratefully acknowledged. Additional computer time was provided by the HHLR Darmstadt and the HLRZ Stuttgart.

[1] a) N.N Greenwood, A. Earnshaw, *The Chemistry of the Elements*, **1997**, VCH, Weinheim; b) K. P. Huber, G. Herzberg in *Molecular Spectra and Molecular Structure, IV. Constants of Diatomic molecules, Vol. 4*, **1979**, Van Nostrand Reinhold Company, New York.

[2] a) A. S. Foust, M. S. Foster, L. F. Dahl, *J. Am. Chem. Soc.* **1969**, *91* 5633; b) G. Huttner, U. Weber, B. Sigwarth, O. Scheidsteger, *Angew. Chem.* **1982**, *94,* 210; *Angew. Chem. Int. Ed. Engl.* **1982**, *21,* 215; *Angew. Chem. Suppl.* **1982**, 411; c) G. Huttner, U. Weber, L. Zsolnai, *Z. Naturforsch.* **1982**, *37b*, 707; d) G. Huttner, B. Sigwarth, O. Scheidsteger, L. Zsolnai, O. Orama *Organometallics* **1985**, *4*, 326; e) B. Sigwarth, L. Zsolnai, H. Berke, G. Huttner, *J. Organomet. Chem.* **1982**, *226*, C5; f) P. J. Sullivan, A. L. Rheingold, *Organometallics* **1982**, *1*, 1547; g) L. Yoong Goh, R. C. Wong, W.-H. Yip, T. C. W. Mak, *Organometallics* **1991**, *10*, 875; h) W. J. Evans, S. L. Gonzales, J. W. Ziller, *J. Am. Chem. Soc.* **1991**, *113*, 9880; i) L. Yoong Goh, W. Chen, R. C. Wong, *J. Organomet. Chem.* **1995**, *503*, 47.

[3] A. D. Allen, F. Bottomley, *Accounts Chem. Res.* **1968**, *1*, 360.

[4] See for example a) P. W. Jolly, K. Jonas, C. Krüger, Y.-H. Tsay *J. Organomet. Chem.* **1971**, *33,* 109. b) R. Sanner, D. M. Duggan, T. C. McKenzie, R. E. Marsh, J. E. Bercaw *J. Am. Chem. Soc.* **1976**, *98*,

8351. c) M. D. Fryzuk, T. S. Haddad, M. Mylvaganam, D. H. McConville, S. J. Rettig *J. Am. Chem. Soc.* **1993**, *115*, 2782.
[5] J. N. Armor, H. Taube, *J. Am. Chem. Soc.* **1970**, *92*, 2560.
[6] D. V. Fomitchev, K. A. Bagley, P. Coppens *J. Am. Chem. Soc.* **2000**, *122*, 532.
[7] See for example: C. Krüger, Y.-H. Tsay, *Angew. Chem.* **1973**, *85*, 1050; *Angew. Chem. Int. Ed. Engl.* **1973**, *12*, 998.
[8] A. S. Foust, C. F. Campana, J. D. Sinclair, L. F. Dahl *Inorg. Chem.* **1979**, *18*, 3047.
[9] C. F. Campana, A. Vizi-Orosz, G. Palyi, L. Markó, L. F. Dahl, *Inorg. Chem.* **1979**, *18*, 3054.
[10] P. Rutsch, G. Huttner, *Angew. Chem.* **2000**, *112,* 3852; *Angew. Chem. Int. Ed. Engl.* **2000**, *39*, 3697.
[11] A. Kovacs, G. Frenking, *Organometallics* **2001**, *20*, 2510.
[12] A. D. Becke, *Phys. Rev. A* **1988**, *38*, 3098.
[13] A. D. Perdew, *Phys. Rev. B* **1986**, *33*, 8822.
[14] Gaussian 98 (Revision A.7), M. J. Frisch, G. W. Trucks, H. B. Schlegel, G. E. Scuseria, M. A. Robb, J. R. Cheeseman, V. G. Zakrzewski, J. A. Montgomery, Jr., R. E. Stratmann, J. C. Burant, S. Dapprich, J. M. Millam, A. D. Daniels, K. N. Kudin, M. C. Strain, O. Farkas, J. Tomasi, V. Barone, M. Cossi, R. Cammi, B. Mennucci, C. Pomelli, C. Adamo, S. Clifford, J. Ochterski, G. A. Petersson, P. Y. Ayala, Q. Cui, K. Morokuma, D. K. Malick, A. D. Rabuck, K. Raghavachari, J. B. Foresman, J. Cioslowski, J. V. Ortiz, A. G. Baboul, B. B. Stefanov, G. Liu, A. Liashenko, P. Piskorz, I. Komaromi, R. Gomperts, R. L. Martin, D. J. Fox, T. Keith, M. A. Al-Laham, C. Y. Peng, A. Nanayakkara, C. Gonzalez, M. Challacombe, P. M. W. Gill, B. G. Johnson, W. Chen, M. W. Wong, J. L. Andres, M. Head-Gordon, E. S. Replogle, and J. A. Pople, Gaussian, Inc., Pittsburgh PA, **1998**.
[15] a) F. M.Bickelhaupt, E. J.Baerends in *Reviews in Computational Chemistry Vol .15* (Eds.: K. B.Lipkowitz, D. B.Boyd), Wiley, New York, **2000**, p. 1; b) G. te Velde, F. M. Bickelhaupt, E. J. Baerends, S. J. A. van Gisbergen, C. Fonseca Guerra, J. G. Snijders, T. Ziegler, *J. Comput. Chem.* **2001**, *22*, 931.
[16] a) P. J. Hay, W. R. Wadt, *J. Chem. Phys.* **1985**, *82*, 270; b) W. R. Wadt, P. J. Hay, *J. Chem. Phys.* **1985**, *82*, 284; c) P. J. Hay, W. R. Wadt, *J. Chem. Phys.* **1985**, *82*, 299.
[17] a) A. Bergner, M. Dolg, W. Kuechle, H. Stoll, H. Preuss, *Mol. Phys.* **1993**, *80*, 1431; b) W. Kuechle, M. Dolg, H. Stoll, H. Preuss, *Mol. Phys.* **1991**, *74*, 1245.
[18] S. Huzinaga, J. Anzelm, M. Klobukowski, E. Radzio-Andzelm, Y. Sakai, H. Tatewaki in *Gaussian Basis Sets for Molecular Calculations*, Elsevier, Amsterdam, **1984**.
[19] Basis sets were obtained from the Extensible Computational Chemistry Environment Basis Set Database, Version 7/30/02, as developed and distributed by the Molecular Science Computing Facility, Environmental and Molecular Sciences Laboratory which is part of the Pacific Northwest Laboratory, P. O. Box 999, Richland, Washington 99352, USA.
[20] A. Höllwarth, M. Böhme, S. Dapprich, A. W. Ehlers, A. Gobbi, V. Jonas, K. F. Köhler, R. Stegmann, A. Veldkamp, G. Frenking, *Chem. Phys. Lett.* **1993**, *208*, 237.
[21] T. J. Lee, H. F. Schaefer III, *J. Chem. Phys.* **1985**, *83*, 1784.
[22] a) J. G. Snijders, *Mol. Phys.* **1978**, *36*, 1789. b) J. G. Snijders, P. Ros, *Mol. Phys.* **1979**, *38*, 1909; c) J. G. Snijders, E. J. Baerends, P. Vernooijs, *At. Data Nucl. Data Tables* **1982**, *26*, 483.
[23] J. G. Guan, P. Duffy, J. T. Carter, D. P. Chong, K. C. Casida, M. E. Casida, M. Wrinn, *J. Chem. Phys.* **1993**, *98*, 4753.
[24] A. E. Reed, L. A. Curtiss, F. Weinhold, *Chem. Rev.* **1988**, *88*, 899.
[25] K. P. Huber and G. Herzberg, *Constants of Diatomic Molecules* (data prepared by J. W. Gallagher and R. D. Johnson, III) in NIST Chemistry WebBook, NIST Standard Reference Database Number 69, Eds. P. J. Linstrom and W. G. Mallard, July 2001, National Institute of Standards and Technology, Gaithersburg MD, 20899 (http://webbook.nist.gov).
[26] H. Sontag, R. Weber *J. Mol. Spectrosc.* **1982**, *91*, 72.
[27] M. O. Sinnokrot, C. D. Sherrill *J. Chem. Phys.* **2001**, *115*, 2439.
[28] F. A. Cotton, A. H. Cowley, X. Feng *J. Am. Chem. Soc.* **1998**, *120*, 1795.
[29] K. Balasubramanian *Chem. Rev.* **1990**, *90*, 93.
[30] F. H. Allen, O. Kennard *Chemical Design Automation News* **1993**, *8*, 1 & 31.
[31] J. R.Harper, A. L.Rheingold *J.Organomet.Chem.* **1990**, *C36*, 390.
[32] a) M. J. S. Dewar, *Bull. Soc. Chim. Fr.,* **1951**, *18*, C71. b) J. Chatt, L. A. Duncanson *J. Chem. Soc.* **1953**, 2939.
[33] S. Sakaki, K. Morokuma, K. Ohkubo *J. Am. Chem. Soc.* **1985**, *107*, 2686.
[34] M. A. Spackman, E. N. Maslen *J. Phys. Chem.* **1986**, *90*, 2020.
[35] a) J. Uddin, G. Frenking, *J. Am. Chem. Soc.* **2001**, *123*, 1683; b) G. Frenking, K. Wichmann, N. Fröhlich, C. Loschen, M. Lein, J. Frunzke, V. M. Rayón, *Coord. Chem. Rev.* **2003**, *238–239*, 55.

Received: January 9, 2003 [F4723]

